Effect of matrix self-healing on the bond-slip behavior of micro steel fibers in ultra-high-performance concrete

Al-Obaidi, Salam; He, Shan; Schlangen, Erik; Ferrara, Liberato

DOI
10.1617/s11527-023-02250-5

Publication date
2023

Document Version
Final published version

Published in
Materials and Structures/Materiaux et Constructions

Materials and Structures (2023)56:161
https://doi.org/10.1617/s11527-023-02250-5

ORIGINAL ARTICLE

Effect of matrix self-healing on the bond-slip behavior of micro steel fibers in ultra-high-performance concrete

Salam Al-Obaidi · Shan He · Erik Schlangen · Liberato Ferrara

Received: 20 April 2023 / Accepted: 18 September 2023

Abstract This study investigates the bond-slip behavior of micro steel fibers embedded into an Ultra-High-Performance Concrete (UHPC) matrix as affected by the self-healing of the same matrix in different exposure conditions. The UHPC matrix contains a crystalline admixture as a promoter of the autogenous self-healing specially added to enhance the durability in the cracked state. For the aforesaid purpose, some samples were partially pre-damaged with controlled preload (fiber pre-slip at different levels) and subjected to one-month exposure in 3.5% NaCl aqueous solution and in tap water to study the fiber corrosion, if any, and the effects of self-healing; after that, they were subjected to a pull-out test, to be compared with the behavior of analogous non-pre-slipped samples undergoing the same curing history. Moreover, some samples were cured in the chloride solution, intended to simulate a marine environment, to study the effect of marine curing on the pull-out behavior of steel fiber. The steel fiber corrosion and self-healing products attached to the surface of the steel fiber were analyzed via Scanning Electron Microscopy (SEM), and Energy -Dispersive Spectroscopy (EDS). The results indicate that the newly healed particles formed on the highly damaged fiber-matrix interface significantly enhance the friction phase of the bond-slip behavior and result in a significant residual capacity compared to non-pre-slipped specimens. On the other hand, the self-healing effect in specimens subjected to low damage pre-slip contributed more to the chemical adhesion region of the bond-slip behavior. Owning to the dense microstructure of the matrix, curing in 3.5% NaCl aqueous solution was not found to significantly affect the pull-out resistance as compared to the samples cured in tap water.

Keywords Bond-slip behavior of steel fibers · Self-healing · UHPFRC composites · Steel fiber corrosion

S. Al-Obaidi (✉) · L. Ferrara
Department of Civil and Environmental Engineering, Politecnico Di Milano, Piazza Leonardo DaVinci 32, 20133 Milan, Italy
e-mail: salammaytham.alobaidi@polimi.it

S. Al-Obaidi
Roads and Transportations Engineering Department, University of Al-Qadisiyah, Diwaniyah 58001, Iraq

S. Al-Obaidi · S. He · E. Schlangen
Department of Civil Engineering and Geoscience, Delft University of Technology, 2628, CN, Delft, The Netherlands

Published online: 11 October 2023

1 Introduction

Steel fibers are used as dispersed reinforcement in cementitious composites to improve the through-crack stress transfer capacity and hence enhance the toughness of the materials under tensile and flexural stresses. Therefore, in the cracked stage, the tensile

and flexural behavior of the composites are dependent on the efficiency of the bond-slip behavior of steel fiber, as well as on the fiber dispersion and orientation with respect to the applied stress.

The impact of the steel fiber-matrix interface bond behavior extends to the durability of the materials at the micromechanical level. The superior durability of uncracked UHPC materials has been proved by several authors [1–4]. Pyo et al. [2] reported a chloride depth of less than 1mm in UHPC after one exposure to 10 wt.% NaCl solution without degradation in the strength performance. However, the durability of cracked UHPC and its link with the behavior of steel fibers inside the cracked region, as affected by the exposure conditions are still under investigation [5–7]. Hashimoto et al. [6] Reported that when UHPC cracked with 0.5 mmm, the chloride ions penetrated deeply and caused corrosion in the steel fibers. On the other hand, Yoo et al. [8] reported that UHPC containing 2% steel fiber showed improvement in performance in terms of tensile strength after corrosion initiation in the steel fiber surface which was attributed to the roughness due to the formation of Ferric Oxide (Fe_2O_3). Shin and Yoo [7] have reported that only when the corrosion degree of steel fibers is moderate the multi-cracked UHPC is showing improvement in the tensile performance. They also attributed the corrosion initiation to the oxidization of the steel fiber after the permeating of NaCl solution into the matrix and reaching the steel fiber. Furthermore, they reported that energy absorption capacity is more influenced by fiber corrosion than tensile strength.

Some studies have shown the effects of corrosion on pre-slipped steel fibers embedded in a UHPC matrix. The straight smooth and corroded steel fibers with 0.3 mm diameter and 30 mm length were investigated, where an increase of the pullout load was reported after twenty weeks of exposure in a chloride environment for low-level preload specimens (0.15 mm slip). However, for high-level preloaded specimens (0.5 mm slip), rupture of the steel fiber was experienced at the cracked region (exposed steel fiber) or at the fiber-matrix interface where severe damage was induced by the same slippage [9, 10]. Furthermore, the same studies showed via microscopic observations that the increase in the toughness and energy of the pullout response was attributable and could be correlated to the corrosion degree and the resulting roughness of the steel fiber surface. The same observation was reported on hooked and double hooked ends steel fibers with a length of 60mm and a diameter of 0.75 mm embedded in an ordinary Steel Fiber Reinforced Concrete, SFRC matrix, where the increase in the fiber-matrix bond in partially pre-slipped specimens subjected to six months of wet-dry cycles (two days each) in 7% concentration chloride aqueous solution was observed [11]. Most of the research concerning the durability investigations of the UHPC has been so far carried out based on 4 Point Bending, 4pb test, or direct tensile test of UHPC specimens, where the chemical substances are transported inside the cracks and reach the steel fibers bridging the crack. The common scenario of steel fiber corrosion starts with the ingress of the chemical substances combined with gas, which alters the pH and RH of the crack surface and eventually causes pitting corrosion of the steel fiber inside the cracks [12]. Chlorides can penetrate through the cement paste and when the concentration reaches the threshold, it can form Friedels's or Kuzel's salt, which in turns alters the microstructure of the cement paste, Chlorides can also accumulate by physical binding in calcium silicate hydrates (C-S–H) [13]. It is worth remarking that the corrosion progress could be decreased over time with the ongoing reactivity of the un-hydrated cement at the crack walls, besides sealing the crack, which could also result in a chloride binding effect [14]. However, the local deterioration mechanism can reach the steel fiber-matrix interface and make the degradation phenomena aggravated, and eventually damage the steel fiber-matrix interface resistance, which could severely impact the UHPC long-term performance [5]. De Weerdt et al. [13] stated that leaching is the main dominant degradation in cement-based materials exposed to any kind of solution. However, the presence of carbonates and sulfates increases and accelerates the leaching degradation mechanism, while the presence of the chlorides has less influence on the leaching's intensity. The limited data cannot confirm such an argument. On the other hand, some researchers have anyway shown that the autogenous self-healing of the cementitious materials could restore part or all of the capacity of the damaged interfaces and cracks under certain exposure conditions and crack opening thresholds [15–23]. This could represent an interesting solution to the development of durable and sustainable materials for

several infrastructure applications that mainly involve exposure to chemical aggressive, marine environment, and/or deicing salts. Banthia and Foy [24] observed an increase in the bond strength of steel fiber after three months of curring in the standard marine environment. Although steel fibers are less vulnerable to corrosion when compared to steel rebars [25], Marcos-Meson et al. [12] has pointed out that the degradation mechanisms observed in the cement matrix at the cracked Steel Fiber Reinforced Concrete, SFRC can dominate its long-term degradation when exposed to corrosive environments such as chlorides and CO_2. Therefore, the corrosion resistance of steel fiber and its impact on the fiber-matrix interface performance needs to be further investigated particularly when a large amount of steel fibers are incorporated in the UHPC mixes. This study has originated in the framework of the two European Commission projects: ReSHEALience (GA 760824), and the Marie Slodowska Curie ITN SMARTINCS (GA 860006), whose objectives were enhancing the durability of high-performance cement-based materials in the cracked state also by incorporating micro- and nano-scale constituents, to formulate/validate a methodology for the durability-based design of UHPC structures in extremely aggressive scenarios, and developing and modelling innovative self-healing strategies for bulk and local application, including optimization of mix designs and development of multi-functional self-healing agents with attention to cost, applicability, and environmental impact respectively. The study was also fostered by the IDEA League Research Stay Program for research cooperation between Politecnico di Milano and the Technical University of Delft. First, it is aiming to investigate the pullout behavior of the micro steel fibers (20 mm long and 0.22 mm in diameter) embedded in a UHPC matrix enhanced with crystalline admixture and exposed to a chloride environment (3.5% NaCl solution) and assess the effects of autogenous self-healing of the UHPC under curing/exposure conditions. Steel fiber pullout test can provide crucial information to understand the macroscopic behavior of the fiber-reinforced composite, further serving as a tool for studying the durability aspects of UHPC. Any deterioration or improvement of the bond-slip relationship due to corrosion or healing effects can reflect on the overall behavior of UHPC structural elements [6, 10]. To this purpose, in this investigation, steel fibers were embedded inside UHPC specimens, and their monotonic pull-out behavior was first investigated as a reference. For further companion samples, fibers were pulled out partially from the matrix, at two different levels of pre-slip, then immersed either in tap water or in a 3.5% NaCl solution to study the effect of the healing and corrosion, if any, up to one-month exposure. Discrimination about healing and degradation effects was also made possible thanks to testing non-pre-slipped specimens which underwent the same curing history as the pre-slipped specimens above. This also provided information about the effects of marine curing on the pullout behavior by curing the samples in 3.5% NaCl solution for one and two months. The investigation was finally complemented with energy dispersive X-ray spectroscopy mapping on scanning electron microscopy image, to assess the nature of the self-healing products and corrosion roughness on the steel fibers extracted from the UHPC matrices after completion of the pull-out tests as abovementioned.

2 Materials

The investigated UHPC matrix is reported in Table 1, the matrix is containing a crystalline admixture (CA) as a self-healing stimulator [26]. Type I Portland cement (PC) and slag (BFS) were used as binder materials whose compositions are detailed in Table 2; the water-to-binder ratio was set to 0.18. The crystalline admixtures are characterized by irregularly shaped particles ranging between 1 to 20 µm. the additive contains oxides of calcium, oxygen, silicon, magnesium, aluminum, and potassium as reported in Table 2. The admixture contributes to refining the pore structure of the composite and therefore enhances the

Table 1 Mix design of the employed UHPC matrices

Constituents	XA-CA
CEM I 52,5 R (kg/m^3)	600
Slag (kg/m^3)	500
Water (liter/m^3)	200
Sand 0–2 mm (kg/m^3)	982
Superplasticizer Glenium ACE 300 ® (liter/m^3)	33
Crystalline Admixture Penetron Admix ® (kg/m^3)	4.8

Table 2 Chemical composition of the employed cement, slag, and crystalline admixture (CA), (LOI: loss on ignition @1000 °C

Oxide (wt.%)	CaO	SiO_2	Al_2O_3	MgO	SO_3	Fe_2O_3	TiO_2	Mn_2O_3	K_2O	Na_2O	Other	LOI
PC	59.7	19.5	4.9	3.3	3.4	3.5	0.2	0.1	0.8	0.2	0.4	2.5
BFS	39.2	38.9	10.2	6.4	1.3	0.4	0.6	0.3	0.5	0.8	0.3	1.2
CA[37]	47.26	13.48	3.70	3.54	2.05	1.44	–	–	0.74	11.02	–	16.77

durability of the materials in the uncracked state as well [27]. Silica sand with a maximum 2mm grain size was used as an aggregate. To achieve a self-consolidating and self-leveling consistency, 33 L/ m^3 polycarboxylate superplasticizer was used. This UHPC mix was proposed in the framework of the ReSHEALience project and its mechanical, durability, and healing performance was thoroughly characterized as reported in [27–35].

Straight steel fibers commercially known as "Azichem Ready Mesh 200®" were used as dispersed reinforcement (which were the same fibers used in the overall experimental activities of the ReSHEALience project in the experimental and real scale application of the investigated UHPCs) [30, 31, 36]. The employed steel fibers are straight and smooth and covered with a brass coating layer; the geometrical and mechanical properties are indicated in Table 3, the latter have been experimentally determined in this investigation on two fiber samples.

3 Experimental programme

To evaluate the bond mechanism of the single steel fiber, UHPC matrix samples with embedded single steel fiber were prepared. Eight steel fibers were positioned in a molded sample at equal distances, four on each side. The mixing protocol reported in Table 4 was followed to mix the UHPC matrix. The UHPC fresh mixture was then poured inside the mold, where steel fibers had been mounted to make the UHPC specimens with 8 steel fibers sticking out. Upon hardening of the UHPC, 24 h later, the specimen was de-molded and immersed either in tap water or 3.5% NaCl solution for curing in the respective scenarios, both at a temperature of 25 ± 2 °C. In total, sixteen specimens were prepared, eight for each curing condition. After one-month curing, the specimens were extracted from the exposure bath and a precise cut was carried out to obtain eight 5 mm thick UHPC samples with steel fiber embedded inside (embedment length = 5 mm) and protruding out of it for the remaining length to be inserted into the pull-out testing device.

Table 4 Mixing protocol

Time (min)	Operation
0–2	Dry mixing of cement, slag, CA, and sand
2–3	Add water, Superplasticizer
4–19	High speed mixing

Four specimens per curing condition were tested after one month, three monotonically up to complete fiber pull-out, and one employed for SEM observation of the fiber surface, as will be later explained in detail. The remaining four specimens already cured in chloride solutions were cured for one more month, to investigate the effects of prolonged aggressive exposure, and then tested as mentioned above. The remaining four specimens cured in tap water were subjected to pre-slip and then healed for one month, two in tap water and two in chloride aqueous solution to investigate the effect of corrosion on the pullout and

Table 3 Steel fiber properties

Diameter (d_f) (mm)	Length (l_f) (mm)	Aspect ratio (d_f/l_f)	Density (g/ cm^3)	YieldTensile strength (MPa)	UltimateTensile strength (MPa)	Elastic modulus (GPa)
0.22	20	90.9	7.85	2250	3066	165

bond strength when steel fiber embedded inside intact and cracked UHPC matrix. At the end of this healing period failure pull-out tests and SEM observations were carried out as later explained in detail. Figure 1 summarizes the complete experimental program carried out in this study.

3.1 Pull-out and pre-slipping tests

A mini-MTS with a maximum capacity of 500 N was used to pull out the single steel fiber from the UHPC matrix specimens, shown in Fig. 2a. The 5mm thick UHPC sample with single steel fiber sticking out has been prepared with a gripping system at both ends as shown in Fig. 2b and c. The specimen with the gripping system then was inserted in the testing machine, where the grips were fixed on both sides of the machine, and a pullout test was performed under displacement control, at a 0.015 mm/s slip rate; the load was registered by the load cell attached to the cross head of the machine and the slippage was recorded via the LVDT installed with the machine (Fig. 2a). By neglecting the elastic deformation of the gripping system, 5 mm exposed steel fiber, 5 mm UHPC matrix, and the loading system, the load-slip curves of the single steel fiber can be obtained by the load cell and LVDT measurements. To evaluate the healing capacity of the UHPC matrix at the interfacial zone between the steel fiber and the matrix, for four specimens cured one month in tap water as illustrated above, steel fibers were pulled out partially to induce controlled damage. These intentional damages were different for each specimen since it was difficult to control the precise slip amount to be the same for all specimens due to the inherent differences in each specimen. Therefore, the preloaded specimens have residual slips ranging from 0.15 mm to 0.3 mm and maximum pullout force ranging from 30 to 35 N. Nevertheless, the response of these preloaded specimens was later compared with the full pullout-slip curve of the same sample to evaluate the improvement or the degradation process associated with each damage. After the induced damage, the specimens were immersed in tap water and 3.5% NaCl solution for one month to examine the autogenous self-healing capacity of the matrix-fiber interface as explained earlier and detailed in Fig. 1. Upon the completion of the exposure duration, each specimen was retrieved from the exposure and tested again: the fiber was pulled out totally from the matrix and compared to the preloading curve and to the reference curve (cured in tap water).

3.2 Scanning electron microscopy (SEM), and energy -dispersive X-ray (EDX) analysis

This investigation was complemented with SEM/EDX analysis of the fiber surface and of the healing products deposited on it; to perform the SEM/EDX analysis, different fiber extracting methods have been used, namely splitting and pullout methods, to examine the pulling effect on the surface condition. The splitting method consisted of making notches, using a precise cutting machine, on both sides of the matrix; the

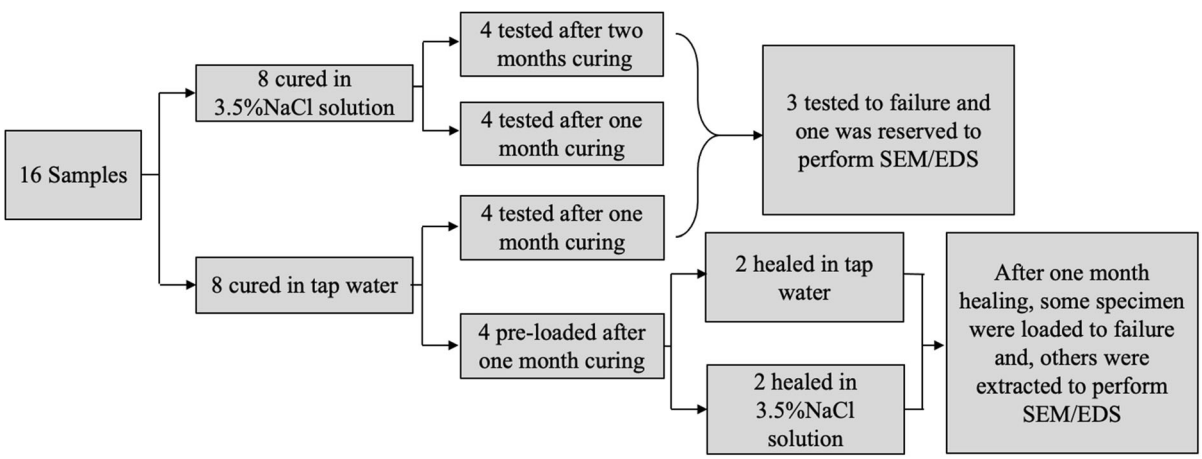

Fig. 1 Flow chart explaining the main layout of the experimental program

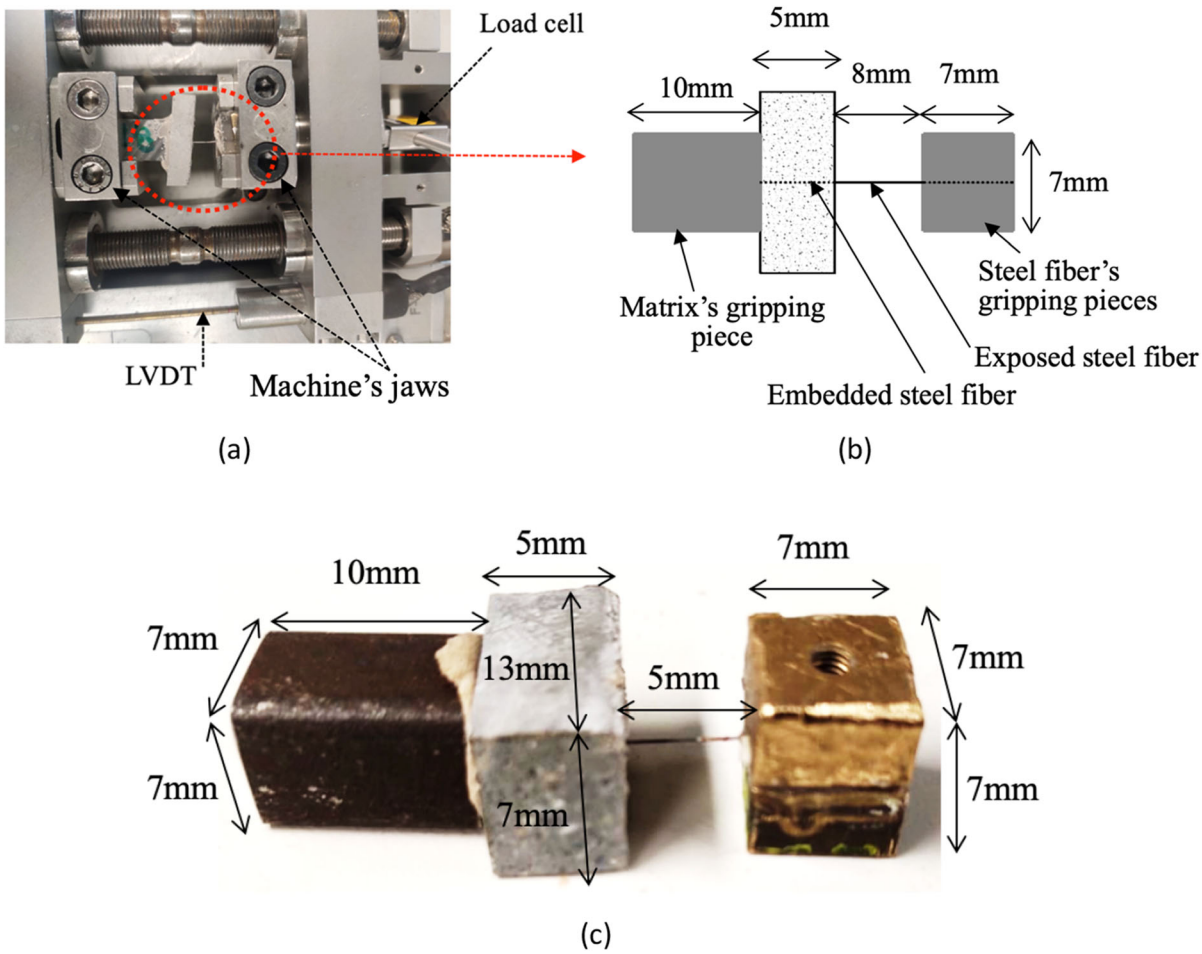

Fig. 2 Test setup: **a** the testing machine, **b** the samples with the gripping system, and c actual picture of the specimens with the gripping setup

notches stopped at the vicinity of the steel fiber, thereafter, a simple pressure was enough to break the matrix and extract the fiber without exterior contamination. SEM analyses were also performed on the fiber as pulled out from the matrix at the end of the pull-out failure tests. It is worth remarking that the SEM observation on the steel fiber extracted by the pullout may not be very informative since the steel fiber has been slipped out through a hard matrix which could affect the surface condition by abrading or wearing out the attached materials on the surface of the steel fiber [9]. However, it will show how the remaining particles (severe corrosion or strongly attached hydrated particles) affect the post-slipping behavior by comparing it with the results of the same analysis done on the fiber that has been extracted by the splitting method. Scanning Electron Microscopy (SEM) was performed on specific steel fibers samples encompassing different exposures and testing

Table 5 Specifications of the specimens of SEM and EDX analysis

No.	Exposure type	Extraction method	
	Non-pre-slipped	Pre-slipped	
1	Water		Splitting
2	NaCl		Splitting
3		Water	Pulled out
4		Water	Pulled out
5		NaCl	Pulled out
6		NaCl	Pulled out

conditions as reported in Table 5. After extracting the samples, they were taken directly to an SEM device equipped with an EDS detector to perform the EDX analysis with the following image data (image and map resolution is 512 by 340, image and map pixel size is 0.4 μm, magnification is 1000, and acceleration voltage is 15 kV). The distribution of the typical chemical elements attached to the extracted steel fiber over selected SEM images is surveyed and reported. The EDX analysis was carried out on SEM images taken in the middle of the embedded length of the steel fiber, i.e., 2.5 mm from the front of the exposed UHPC matrix.

4 Experimental results

4.1 Effect of curing in 3.5% NaCl aqueous solution

One of the objectives of this study is to investigate the effect of curing the UHPC in chloride solution, The idea of curing the samples in standard 3.5%NaCl was to see the influence of the chloride exposure on the steel fiber 24 h after casting. In fact, the concrete materials may engage with the surrounding environments immediately after casting and before reaching their full intended functionality, and sometimes combined with shrinkage cracks that jeopardize the steel fiber or/ and the fiber-matrix pull-out strength and put it in direct exposure to a chloride environment, for this reason, specimens with steel fiber embedded in UHPC matrix were cured either in tap water or 3.5% NaCl solution for one and two months. The specimens were extracted from the exposure after each target period and tested to obtain the bond strength-slip behavior and the influence of the marine environment curing assessed by comparison. Three pullout curves of each test as well as the average curve are presented in Fig. 3, the pullout tests of one month curing in tap water are reported in Fig. 3a, one and two- month curing in 3.5%NaCl aqueous solution are reported in Fig. 3b. In Fig. 4, the pullout load and shear stress versus the slip curves are presented. The shear stress is obtained by dividing the pullout load over the actual residual bonding lateral surface as shown in Eq. 1 [38].

$$\text{Shear stress}(s) = \frac{P(s)}{\pi \times d_f \times (L_e - s)} \quad (1)$$

where: *P(s)* is the pullout load as a function of the slip, d_f is the steel fiber diameter, L_e is the embedded length inside the UHPC matrix, and s is the progressive slip of the steel fiber from the matrix. As shown in Fig. 4, in the initial stage the pullout load increases with very limited slippage, the chemical adhesion and friction between the steel fiber and the surrounding matrix are responsible for the bond development.

Immediately after reaching the peak pullout load, a steep reduction in the force was observed, where the chemical adhesion is lost and only the friction force, which is almost linearly proportional to the slip value, is holding the steel fiber. Therefore, the shear stress is almost constant throughout this stage except when approaching the tip end of the fiber where the deformation from the cutting procedure is believed to increase the friction resisting steeply due to anchorage action [39]. Moreover, the accumulated debris peeled off from the slipping action could form a wedging effect at the end of the fiber [38]. The average bond strength for all materials after one-month exposure to water is about 8 MPa. The specimens cured in the simulated marine environment for one month exhibited an increase of 9 N in the pullout load and 3 MPa in the bond strength after one month of curing in the saline environment. The rate of the increase is about 35% with respect to similar samples cured in tap water for one month.

The same increase rate is also evident in the post-slip phase, where the effect of the friction is clear from the minor fluctuation of the registered data: in fact, during the testing of these samples, the sound of fiber slipping out of the matrix was interestingly noticeable. According to the best knowledge of the authors, the only related study is reported by Banthia and Foy [24], who incorporated micro silica in their mixture and tested the specimens after one month, and three months of curing in both tap water and marine environments with different temperatures: 2 °C, 22 °C, and 38 °C. They reported a higher pullout strength for the specimens cured in the seawater, where they claimed that the artificial and the real seawater contains calcium chloride which promotes the early high strength of the matrix. Some accumulation of a small amount of corrosion substances on the steel fiber surface was also claimed to be the reason for

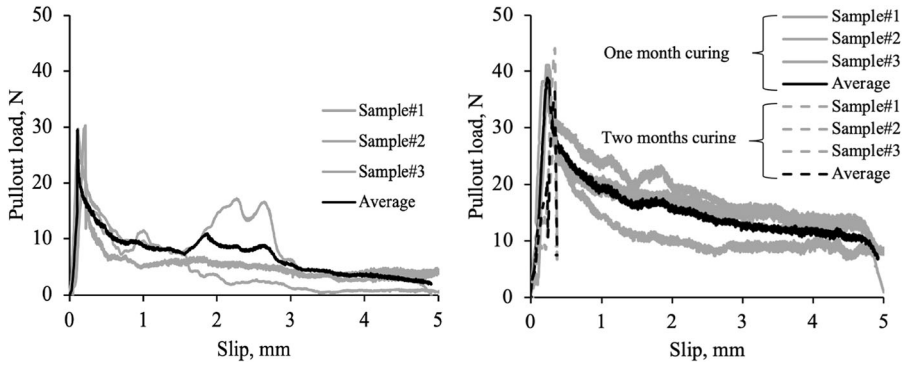

Fig. 3 Pullout loads for specimens; **a** cured in tap water for one month, and **b** cured in 3.5% NaCl aqueous solution for one month and two months

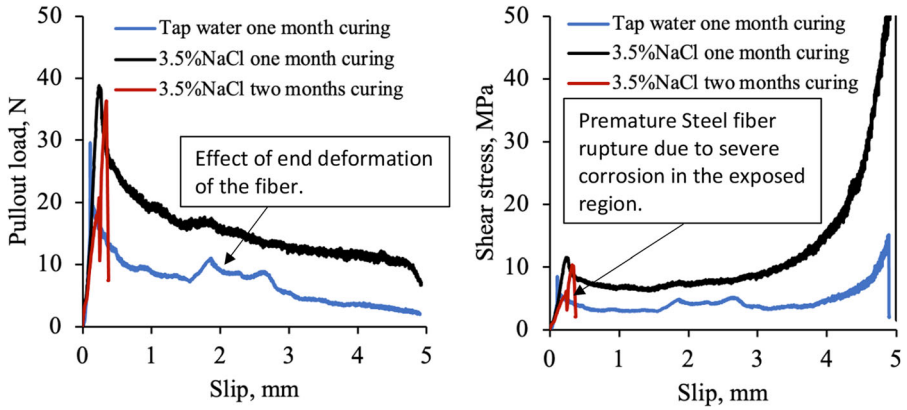

Fig. 4 Comparison of pullout force-slip curves: **a** and pull-out shear stress-slip curves, and **b** after curing in fresh and 3.5 NaCl solution

the pullout increase, whose build-up can exert a confinement pressure on the fiber and result in the pullout strength increase, the same observation was reported by V.Marcos-meson et al. [40, 41]. This favorable feature of corrosion can stay as long as the matrix and steel fiber sustain the stress. Interestingly, Banthia and Foy [24] also found that the pullout force after three months for specimens cured in seawater at 2 °C and 22 °C was higher as compared to that of specimens cured in seawater at 38 °C. This conclusion was supported by the SEM analysis, where they observed that the high temperature promotes earlier faster corrosion and leads to a reduction in the steel fiber cross-section under prolonged exposure as well as impacting the bearing contribution of the bond in the case of the hooked end steel fiber and therefore result in bond strength reduction. On the other hand, the addition of micro silica appeared to have no enhancement against corrosion resistance. In this study, the curing temperature of the laboratory was about 25 °C and since the sticking-out fiber was not protected against direct exposure, after 2 months the specimens exposed to a simulated marine environment experienced premature rupture of the severely corroded steel fiber in the exposed region as shown in Fig. 5.

4.2 Effect of the damage—healing in tap water and 3.5% NaCl solution

As stated above, in order to evaluate the healing capacity of the UHPC matrix at the interfacial zone between the steel fiber and the matrix, after one month of curing in tap water, and for four specimens the steel fibers were pulled out partially to induce some controlled damage. After the induced damage, the specimens were immersed either in tap water or 3.5% NaCl aqueous solution for one month to examine the

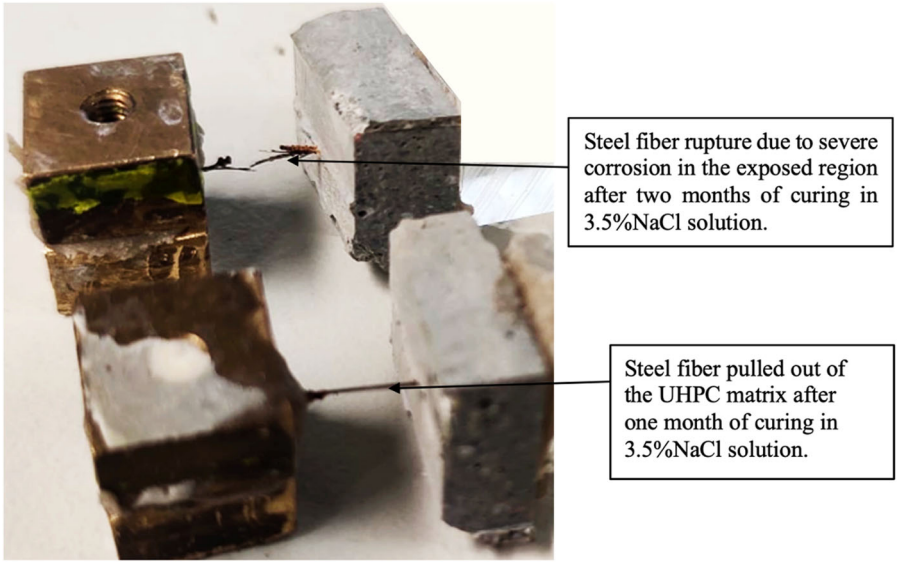

Fig. 5 Failure patterns of the specimens after one month and two months of exposure to the 3.5% NaCl solution

autogenous self-healing capacity of the matrix–fiber interface as explained earlier and detailed in Fig. 1. Upon the completion of the exposure duration, each specimen was retrieved from the exposure and tested again: the fiber was pulled out totally from the matrix and the recorded response was compared to the preloading curve and to the reference curve (companion undamaged specimens cured in tap water or in chloride solution) which are previously reported in Figs. 3 and 4 in the previous section. Figure 6 shows the pullout-slip curves for the specimens preloaded and healed in the tap water for one month and also the comparison with the reference samples, which have not been damaged and healed. In general, the healing effect is clearly and interestingly pronounced. In fact, Fig. 6 shows that the preloading degree was significant: the residual pre-slippage was about 0.3 mm, the preloaded pullout load exceeded the peak value (the adhesive bond was completely lost), and the bond resistance entered the descending phase, where only the frictional bond governs, then the unloading phase takes place. Nonetheless, no sudden drop in the pullout load after reaching the peak value was recorded; this may indicate that the interface between the matrix and the steel fiber for this specimen has been affected due to damage/healing effect and perhaps the friction

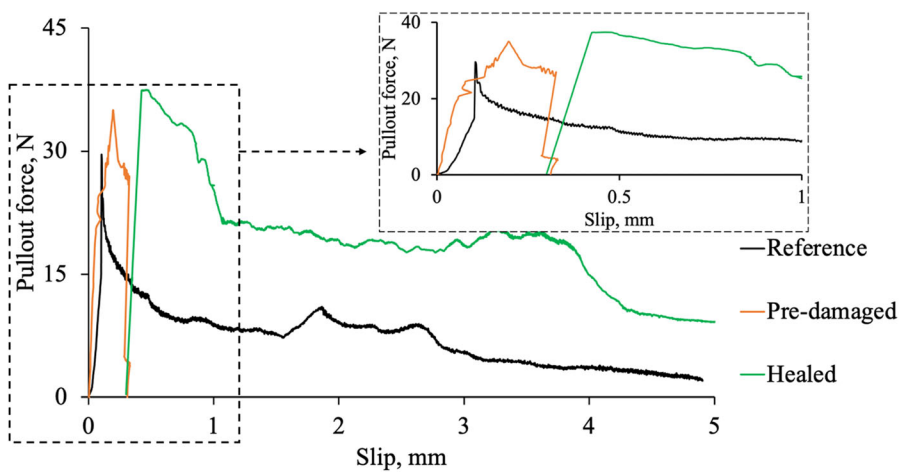

Fig. 6 Comparison of pullout force-slip curves pre-slipped and one month healed in tap water

coefficient and or the steel fiber surface pressure has increased consequently [39]. For the case of the specimen preloaded and healed in 3.5% NaCl for one month, Fig. 7, the same observation of tap water healing condition was obtained. As stated previously, different residual slips were achieved during the preloading process. According to these different damage levels, different healing degrees were obtained. For instance, the specimen in this case has residual slippage of 0.15 mm, with the pre-load value exceeding the peak load, the adhesive bond has completely lost and the matrix-steel fiber interface is damaged, after this point, only the frictional bond is governing, where the performance is softening down to 50% of the peak load.

However, after one month of healing in the 3.5% NaCl aqueous solution, the regain in the pullout load was remarkable, since the specimen was able to recover its full peak load moreover, the post-slippage regime experienced slip hardening behavior, and eventually, the load starts to descend gradually after reaching 2.5 mm slippage [42].

By integrating the area under the pullout load-slip curve the pull-out energy, E_p was calculated based on Eq. 2 [43]. The bond strength between the steel fiber and UHPC matrix is obtained using the results reported in Figs. 4, 6, and 7 as well as fiber geometry i.e., the steel fiber diameter d_f and the embedment length L_e, then based on the pull-out energy, the equivalent bond stress was evaluated as per Eq. 3 and was evaluated based on the pullout energy, E_p assuming the interfacial bond strength constant throughout the entire embedded steel fiber length [9]. However, the average maximum bond stress can be evaluated from Eq. 4, where the maximum pullout force is divided over the entire bond circumference surface area of the embedded fiber. These bond parameters are necessary to understand the bond behavior before and after the maximum pullout load and to compare the results of different curing conditions on different UHPC material types as they are shown in Fig. 8.

$$E_p = \int_0^{L_e} P(s)ds \tag{2}$$

$$\text{Equivalent bond stress} = \frac{2E_p}{\pi \times d_f \times {L_e}^2} \tag{3}$$

$$\text{Avearage maximum bond stress} = \frac{Pmax}{\pi \times d_f \times L_e} \tag{4}$$

It can be observed that the maximum pullout loads and the pullout energy of the healed samples are higher than the reference ones. It is worth highlighting that the increase in the healing efficiency of the preloaded specimens immersed in the water was more pronounced before the debonding of the fiber occurred, i.e., the chemical adhesion bond was enhanced as clearly shown in Fig. 6. The preloaded specimens healed in 3.5% NaCl solution exhibited higher pullout energy than those healed in tap water as shown in Fig. 8a. The same observation has been pointed out by other researchers [7, 9, 12] who claimed that the chloride might have penetrated through the steel fiber-matrix interface and initiated the corrosion which is roughing the surface of the steel fiber and increasing the frictional effect and energy of pulling out.

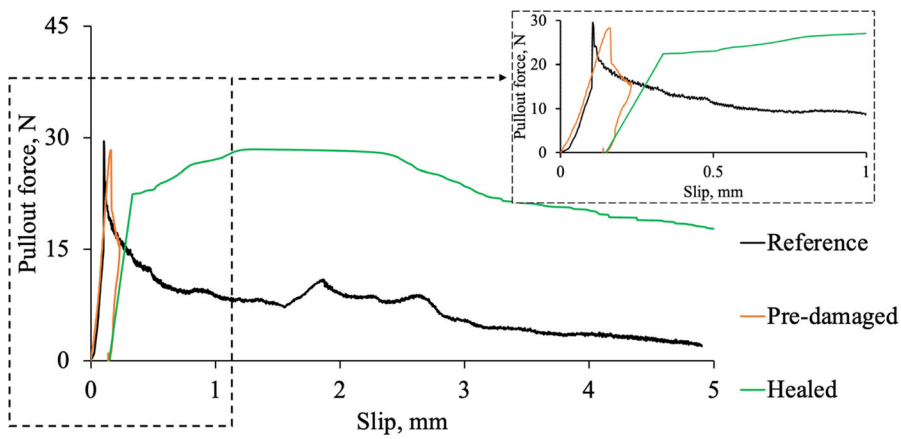

Fig. 7 Comparison of pullout force-slip curves pre-slipped and one month healed in 3.5NaCl solution

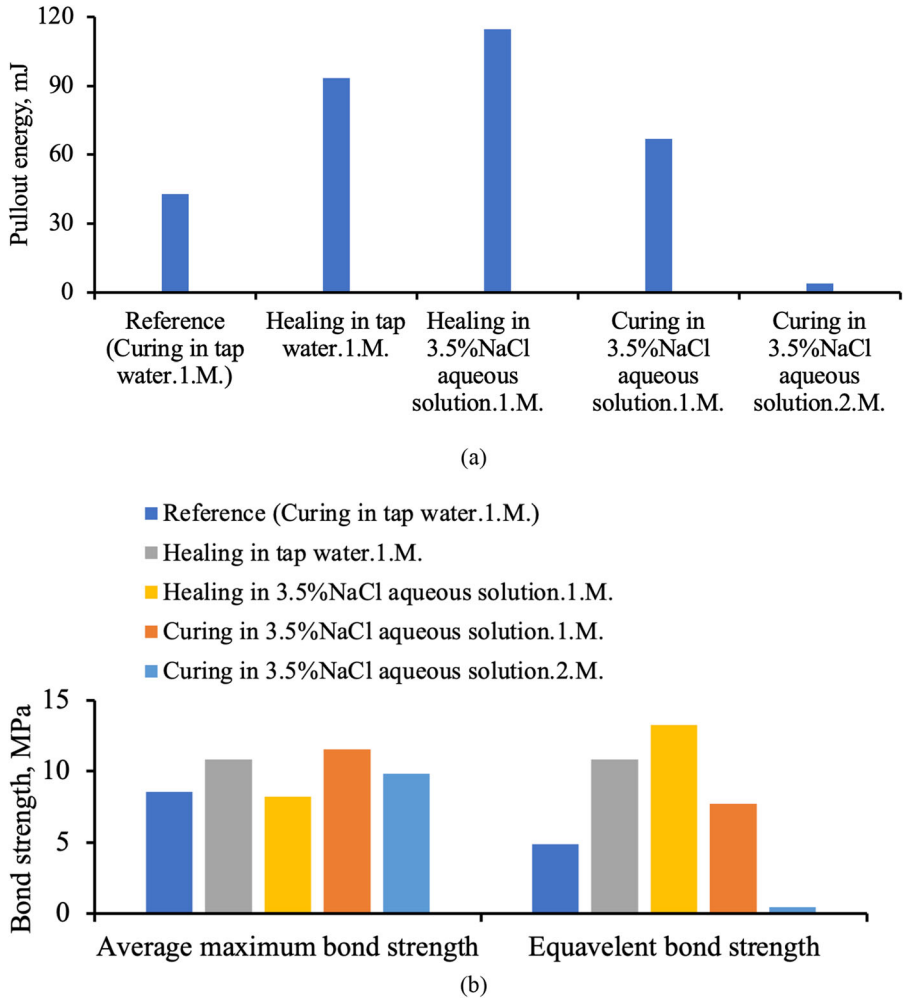

Fig. 8 Pullout-slips parameters for different curing conditions, and healing environments, **a** pullout energy, and **b** bond strength

4.3 Scanning electron microscopy (SEM), and energy -dispersive X-ray (EDX) analysis

As described in Fig. 1, some specimens were saved to conduct SEM and EDX analysis. Figure 9 shows SEM images of the selected steel fiber along the exposed and 5mm embedded regions, the indicated numbers are linked to Table 5 where exposure and extraction method were specified. Due to a lack of useful information and to save time and effort, the SEM analysis was not performed on the full length of the fibers for some samples. Therefore, a discontinuity of the fiber surface morphology is shown for samples 2–6 in Fig. 9. Specimens (1, and 2) were extracted from the matrix by splitting method. Generally, the surface of the fibers contains many debris which could roughen the surface and increase the frictional resistance phase of the pullout. Nonetheless, there is some damage to the fibers due to the extracting methods where the blades of the cutting machine could have hit the fiber on the surface and caused these damages. The end deformation of the fiber due to the manufactural cutting of the steel wire is also clear for the specimens in Fig. 9 [10, 39]. These end deformations are not evident on the fibers that were extracted by the pullout method, where the slipping out through the hard matrix has damaged them and caused the steep increase in the shear-slip curve reported in Fig. 4. On the other hand, the specimens which were extracted by pull-out, are showing less debris or hydration products on their surface where the pulling out through hard matrix has worn out the surface.

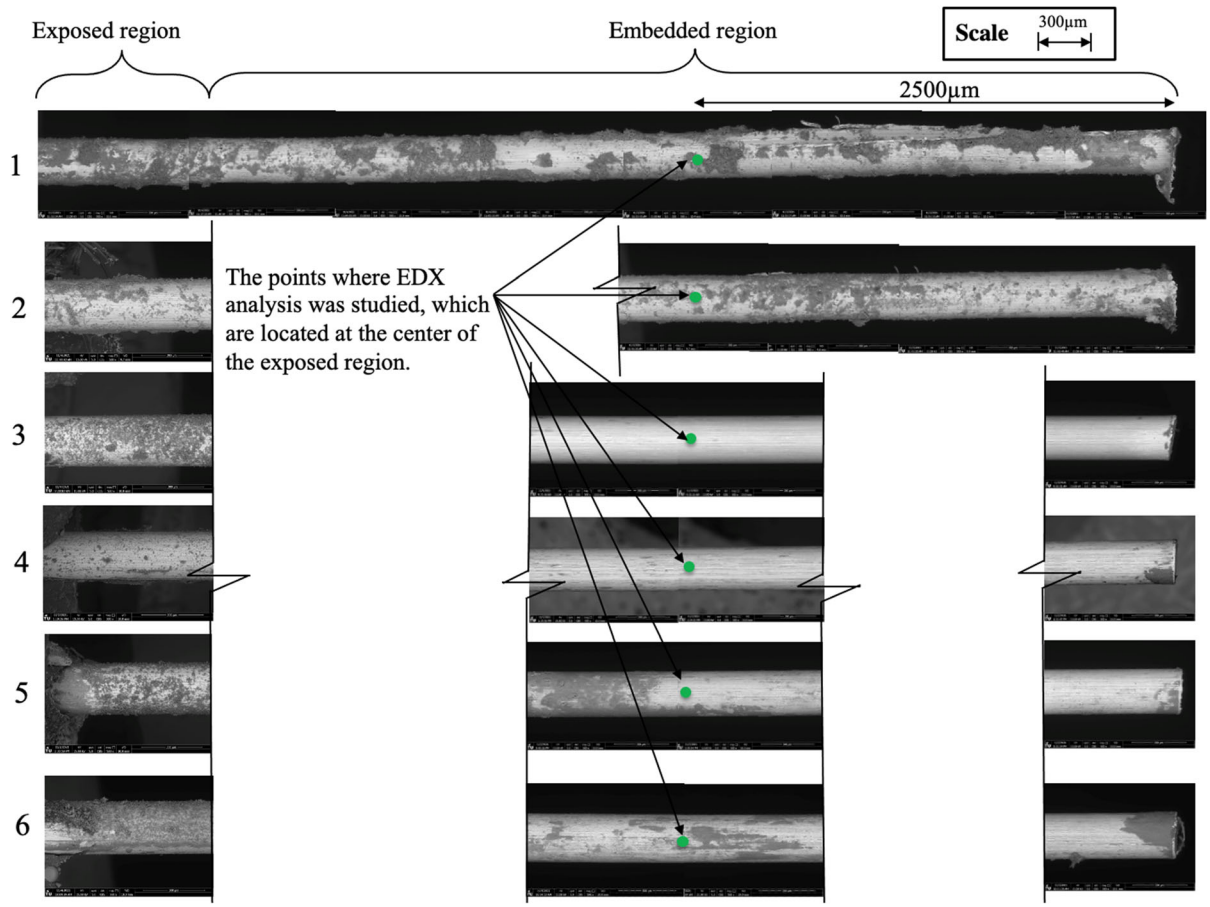

Fig. 9 Microscopic images showing the morphology for the extracted steel fiber specimens by splitting, and pullout methods, the indicated numbers are linked to Table 5 where exposure and extraction method were specified

Nonetheless, specimens (5, and 6) which were immersed in 3.5% NaCl solution are showing more roughness on the surface than the specimens immersed in the freshwater. The embedded steel fiber surfaces of specimens (3, and 4) are relatively clear compared to specimens (5, and 6) indicating no corrosion or delayed hydration particles which are supposed to be abraded through the pulling process of the fiber through the hard matrix. The absence of steel surface roughness in these samples is also an indication that no steel oxidation has occurred in the embedded part of the steel fiber surface. The energy dispersive X-ray (EDX) was performed on the microscope images taken at the mid-point of the embedded steel fiber, i.e., 2.5 mm from the end of the steel fiber for selected specimens to highlight and confirm the role of the experimental variables, Figs. 9 and 10a.

For instance, specimens 1 and 2 were selected to investigate the effect of saltwater curing on the microstructure of the UHPC matrix, where specimen 1 was cured in fresh water and specimen 2 features the same matrix but cured in salt water. Since these samples were exposed to fresh water and salt water respectively and extracted by splitting method, it would make a rational analysis to evaluate the corrosion degrees of steel fiber by EDX spectrum. As can be seen from Fig. 10b, the steel fiber extracted from the matrix that was exposed to the saltwater contains chloride (Cl) elements in the middle of the embedded region. This indicates that the chloride elements have penetrated through the matrix and reached the steel fiber surface at a location of 2.5 mm from the exposed surface.

Moreover, the percentage of the Carbon (C) and Oxygen (O) elements found on the surface of this

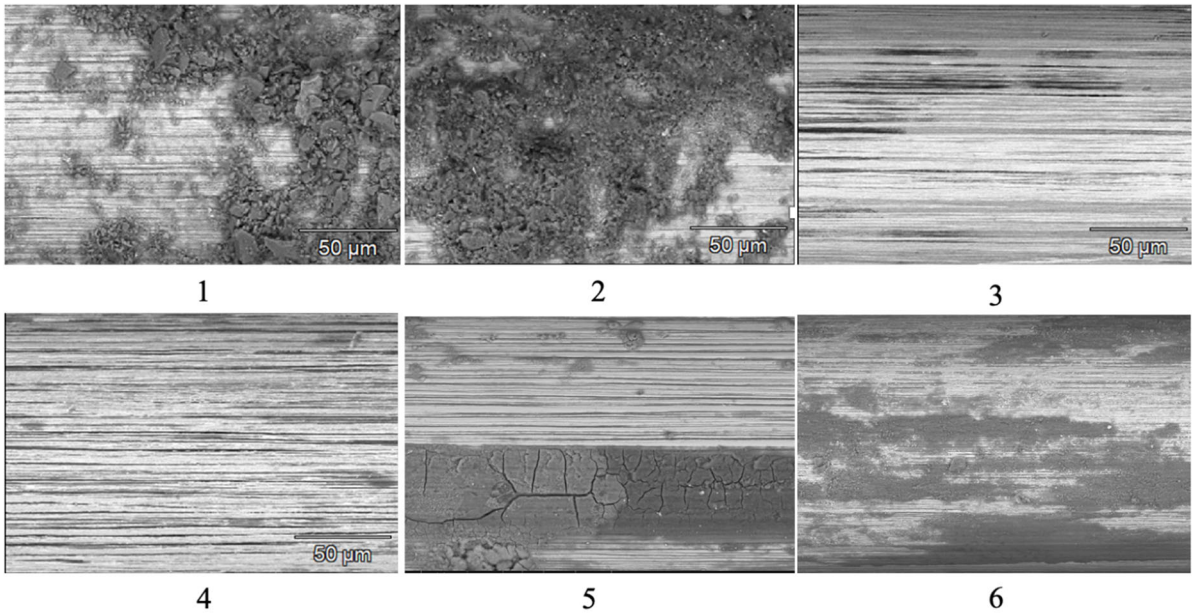

(a)

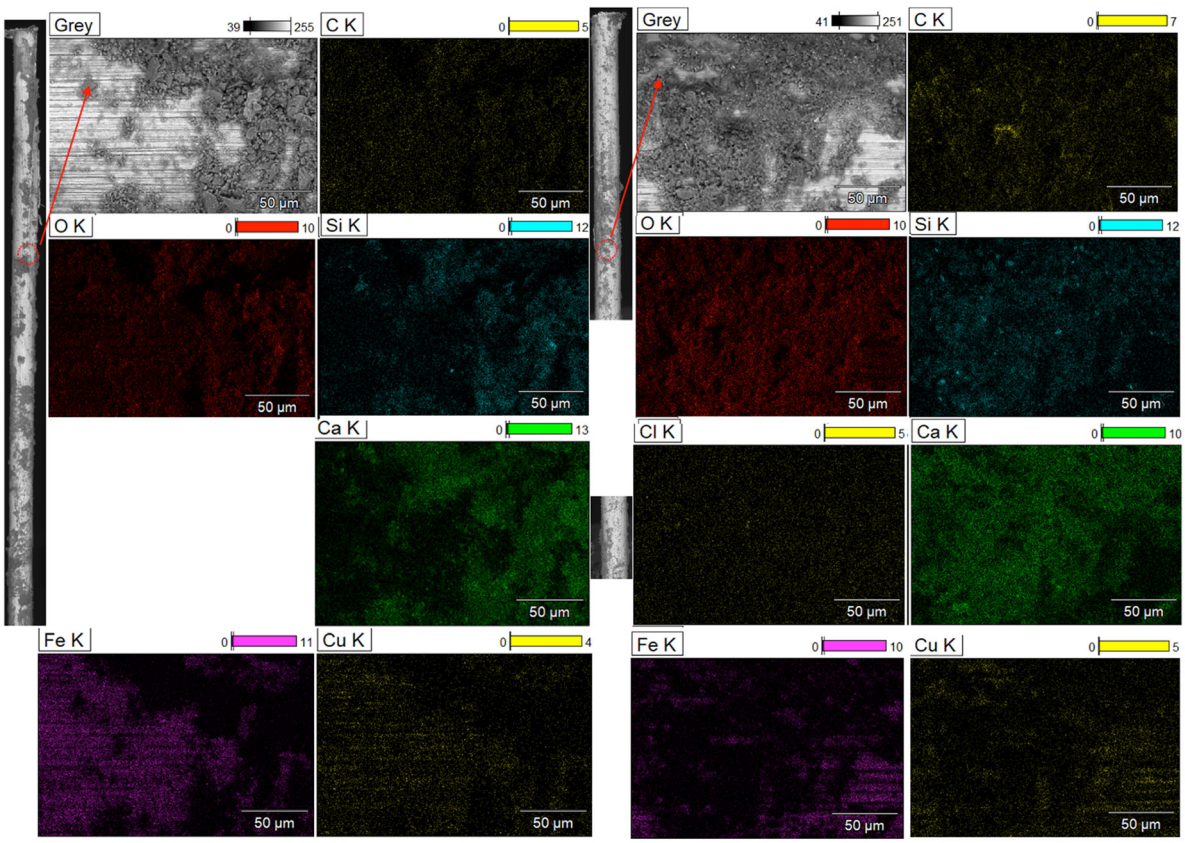

(b)

◀**Fig. 10** SEM/EDX analysis, **a** SEM images selected for EDX analysis, and **b** EDX mapping for sample 1 (left side) and sample 2 (right side) to show the effect of a corrosive environment

sample are more than those found on the samples immersed in fresh water. The presence of Oxygen (O) and iron (Fe) on the surface of these samples and the almost diminished brass-coated Copper (Cu) could indicate the formation of ferric oxide (Fe_2O_3) on the surface of samples 2 [9]. These elements besides the Ca and Si that form Calcium Silicate hydrate, C–S–H contribute to the observed restoration adhesive bond strength and increased frictional bond strength of samples cured and healed in chloride solution in accordance with Naaman and Najm [44], and Oh et al. [45]. The distribution of the typical chemical elements attached to the extracted steel fiber over selected SEM images is surveyed and reported in Fig. 11.

The EDX results reported in Fig. 11, for specimens in the respective order cited above, show the presence of silicon and calcium in all specimens which could be an indication of the calcium-silicate-hydrate C–S–H. On the other hand, the percentage of oxygen is less in the case of the sample cured in the tap water, which could potentially indicate a less formation of ferric oxide (Fe_2O_3) than specimens exposed to salt water. Specimens 3–6 were also selected to study the preloading effect on the interfacial zone between the fiber and the matrix, where specimens3, and 4 have been immersed in the tap water, whereas specimens 5, and 6 have been immersed in chloride solution after the preloading. The analysis shows once again the presence of calcium-silicate-hydrate C–S–H, as a product of the delayed hydration reactions in the tunnel cracks formed at the fiber-matrix interface because of the pre-slip. However, the calcium and silicon in the specimens cured in a saline environment are higher than in the specimen cured in tap water, this well justifies the higher bond capacity obtained by the specimens cured in the salt water, which could also be calcium chlorides formation as an effect of the reaction between chloride and calcium ions, this observation was clearly pointed out by [24] where they claimed that the marine environment contains calcium chloride that could enhance the strength of the matrix.

Specimens 5 and 6 have a higher percentage of oxygen than specimens 3, and 4, which could be an indication of corrosion initiation, which explains the high energy produced from the pulling out of the steel

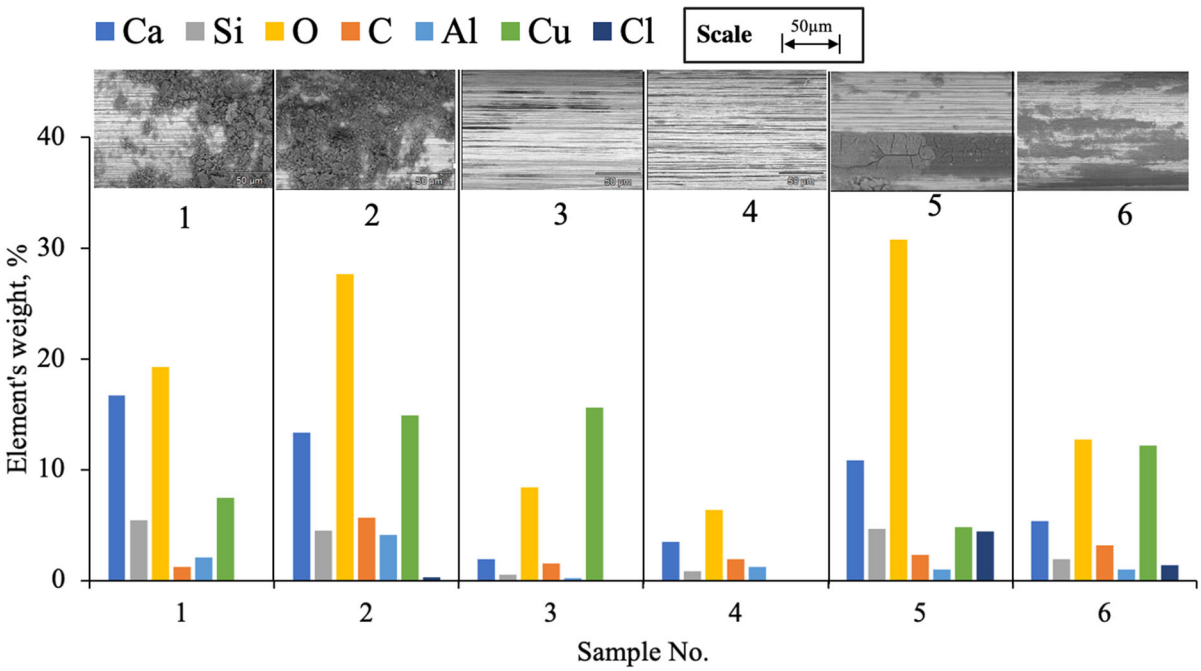

Fig. 11 EDX analysis for the samples (numbers refer to conditions reported in Table 5)

fiber of these specimens. It is furthermore worth mentioning that results of EDX analysis show the elements of Cu on the specimens that are extracted via the splitting method, and on specimens healed in tap water, this element belongs to the brass coating covering the steel fiber, which was worn out during the pull-out and or has been affected by the corrosion initiation.

5 Discussion

The reported results in the previous section show how the damaged/healed fiber-matrix interface performed after being exposed to fresh and saline water. The fiber-matrix interface has restored its capacity after being partially damaged and healed. The obtained results are discussed here to explain the main factors that lead to this behavior. The increase in the pullout load and energy can be attributed to modifications in the interfacial zone between the fiber and the matrix [40], where the reaction of the un-hydrated cement can be engaged and activated [12]. As reported in [46], the microstructure of the interface between the steel fiber and the UHPC matrix is mainly composed of a porous layer consisting of Calcium Hydroxide (CH), C–S–H, and ettringite near the steel fiber surface, this layer becomes denser and denser as it approaches the bulk matrix. During the damage phase, the debonding does not occur exactly at the steel fiber interface but extends to (10–40) μm from the fiber surface depending on the weak layer [47], which can also bring hydrated particles and debris on the surface of the pre-slipped fiber, Fig. 12. Therefore, continuous hydration during the healing period can grow around these particles and form a new interface. Within this newly formed interface, the weak interface moves further away from the fiber, thus increasing the bonding capacity; moreover, the attached particles and debris from the damage phase can work as an interlocking element to enhance the bonding. Nonetheless, based on the results of one month of healing either in tap water or 3.5% NaCl solution, the interface characteristics were completely restored, or perhaps a new interface with different characteristics was formed [23, 40, 48, 49], which resulted into the regain in peak pullout value, as clearly reported in Fig. 6, and in case of Fig. 7. The regaining in the pullout capacity is higher than the peak value, even though the stiffness is decreased for the recovered part.

Owing to the highly densified microstructure of UHPC, Pyo et al. [2] observed an insufficient formation of rust crystals on the surface of the steel fiber, thus adhesive and chemically bonded portion in the damaged fiber-matrix interface was completely filled with hydrates, while the corrosive particles from NaCl solution and formation of Fe_2O_3 could be penetrated through the highly porous interface of the debonding region. Marcos-Meson et al. [11, 41] reported an increase in the maximum pullout force of hooked steel fiber after 1mm preloaded value and wet-dry cycles. Yoo et al. [10] also reported a significant increase of the pullout force (more than twice) which was correlated to the corrosion degree (2–5%) that caused steel surface roughness attributed to Ferric oxide accumulated on the surface of the steel fiber. However, a corrosion degree beyond 5% caused the resistance to decrease due to a reduction in the fiber cross-section and premature rupture. Nonetheless, Marcos-Meson et al. [40] stated that the limited corrosion roughness observed on the embedded region of the steel fiber surface did not contribute to the steel fiber roughness, but they attributed the increase in the adhesive bond strength to the autogenous healing of fiber-matrix interface and accumulation of the corrosion products between the steel fiber and the matrix.

The specimen cured in the 3.5% NaCl solution for one month has also shown an increase in the pullout energy compared to the companion sample cured in fresh water. However, due to the premature rupture of specimens cured in the 3.5% NaCl solution for two months, very low pullout energy is obtained. On the other hand, according to Marcos-Meson et al. [12], the long-term degradation of SFRC in wet-dry cycles combined with chloride and CO_2 exposure can be very complex if interferes with radial microcracks, corrosion of the fiber, and the autogenous self-healing, and thus further research is recommended to study the relationship between these parameters and the bond strength of damaged fiber-matrix interface. It is also worth noting that the percentage of the Cl ions are present in samples 2, 5, and 6, these samples were exposed to chloride solution, but the interesting observation here is that the pre-slipped samples (5, and 6) show more chloride percentage than the intact sample 2. This indicates that the preloading effect has permitted the chloride ions to penetrate deeply into the

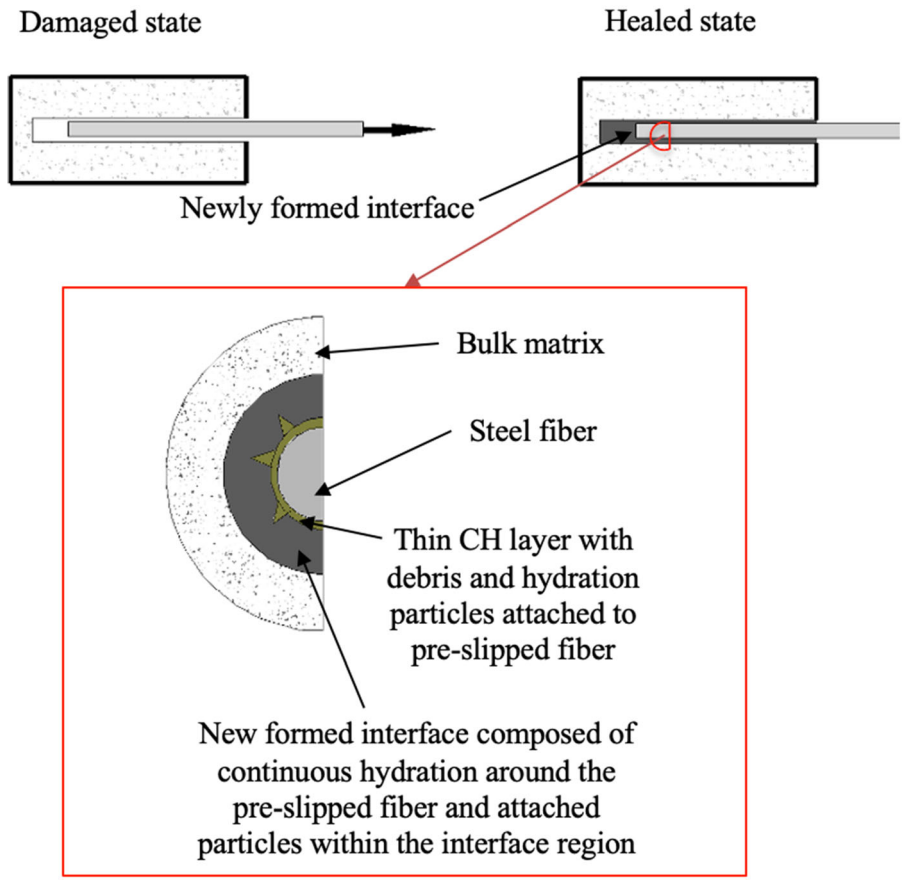

Fig. 12 Schematic bonding mechanism before and after self-healing

matrix and reach the interfacial region at 2.5 mm from the exposed surface, this can be seen from Fig. 10b, specimen 1 was cured in fresh water and specimen 2 features the same matrix but cured in salt water. The steel fiber extracted from the matrix that was exposed to the saltwater contains chloride (Cl) elements in the middle of the embedded region. Also the presence of Oxygen (O) and iron (Fe) on the surface of these samples and the almost diminished brass-coated Copper (Cu) could indicate the formation of ferric oxide (Fe_2O_3) on the surface of sample 2 as was also reported by Yoo et al. [9].

Yoo et al. [10] stated that the initiation of corrosion on the surface of steel fibers enhanced the interfacial bonding strength in UHPC when the fibers were aligned with the pullout force.

The CA can promote the release of Ca_2^+ ions into the crack solution and increases the PH of the Pore solution which as a result accelerates the formation of $CaCO_3$ As reported by Sisomphon et al. [50]. The crystalline admixture has a high tendency to react with cement paste or products of cement hydration and produce newly form of calcium silicate hydrate products since it contains a high amount of calcium and reactive silica, as reported in Table 2, these reactive components can react with the Ca_2^+ to form crystalline or gel products that enhance the interfacial bond strength [50]. It is also worth noting that the percentage of the Cl ions are present in samples 2, 5, and 6, these samples were exposed to chloride solution, but the interesting observation here is that the pre-slipped samples (5, and 6) show more chloride percentage than the intact sample 2. This indicates that the preloading effect has permitted the chloride ions to penetrate deeply into the matrix and reach the interfacial region at 2.5 mm from the exposed surface. It was also pointed out by Marcos-Meson et al. [12] that the leaching of portlandite (CH) in the vicinity of

the cracked matrix could activate the matrix to release OH^- and Ca_2^+ ions. Therefore, the steel fiber-matrix interface was filled with layers of calcite as a fine-grained result of the carbonation process of the CH layer. De Weerdt et al. [13] indicated that leaching is the main degradation scenario of all exposure solutions, the Ca-rich phases can be decalcified and the resulting calcium carbonate and calcium sulfate precipitate at the interface of the cement. They also stated that chloride can accumulate in C–S–H through physical binding. In addition, if chloride ingresses into the cement paste, it can form chloride-containing AFm phases (Friedel's or Kuzel's salt) that alter the microstructure of the cement paste [13]. The bond strength of steel fiber in UHPC was also improved by the presence of $CaCO_3$ precipitated particles on the surface as reported by Kim et al. [51]. The finely grained calcite partially filled the de-bonded region of the fiber-matrix interface, Fig. 12, and could also increase the bonding strength in the UHPC matrix after wet-dry cycles in NaCl aqueous solution [9].

6 Conclusions

In this paper, the steel fiber-UHPC matrix interface bond and the influencing parameters have been assessed by pre-slipping of fibers and subsequent autogenous healing, as also stimulated by crystalline admixtures, both in tap water and aggressive environments represented by a 3.5% NaCl aqueous solution. The interfacial bond performance was evaluated by means of pullout tests accompanied by SEM and EDX observations, to understand the nature of competing phenomena, i.e., self-healing and fiber degradation, if any. Based on the obtained results, the following conclusions can be formulated.

6.1 The effects of the curing environment

- Curing in a chloride environment seems to affect the performance of the UHPC matrix with a noticeable increase in the pullout load and energy. This may be due to the likely presence of calcium chloride formation as an effect of the reaction between chloride and calcium ions, calcium chlorides can promote the early strength development of the matrix. However, this favorable increase in the pullout strength is limited to a slight corrosion degree that alters the roughness of the fiber, whereas the severe corrosion degree can decrease the cross-section of the fiber and lead to premature rupture of the steel fiber.
- To eliminate the premature rupture of the steel fiber and to investigate the long-term performance of salt water curing, a modification on the sample setup should be applied, where the exposed part of the steel fiber should be protected from direct exposure to the chloride environment and different curing temperatures should also be investigated.

6.2 The effects of fiber-matrix interface healing

- The restoration of the adhesive bond reported in the sample healed in the freshwater could be attributed to autogenous self-healing that occurred at the damaged fiber-matrix interface.
- The damage induced on the specimens activated the matrix to produce a new interfacial bonding mechanism, the attached particles and debris or (The finely grained calcite) partially filled de-bonded region can work as an interlocking element to enhance the bonding when the continuous hydration forms around them.
- The formation of early-stage corrosion products on the embedded portion of the fibers due to permeating of the chlorides caused by pre-slipping could also have resulted in the observed improvement of the bond performance, and overall absorbed energy.
- The EDX on SEM analysis indicates the presence of Calcium Silicate hydrates C–S–H on the surface of the steel fibers obtained from the healed specimens in both exposures or Ca_2^+ ions resulting from the leaching of portlandite (CH) in the vicinity of the damaged matrix or from the promotion of CA. However, specimens healed in the chloride exposure revealed the presence of carbon and chlorides or the formation of ferric oxide (Fe_2O_3) on the surface of samples. The formation of these elements and phases could alter the microstructure of the steel-matrix interface and enhance the bonding strength.

The results obtained in this study shed light on the microstructure of the steel fiber-UHPC matrix

interface, where the self-healing of the damaged interface was observed in tap water and aggressive environmental conditions. Therefore, the observed micromechanical enhancement can be further integrated and upgraded to meso-and macro-levels to account for the effects of self-repairing functionalities of UHPC on its long-term mechanical and structural performance in the framework of a durability-performance-based design approach. This could also open tailored long-term experimental campaigns in the framework of dedicated research lines to quantify the healing, and corrosion degree at the fiber-matrix interface and correlate them to the pullout performance and integrate these micro- and mesoscale findings into the macroscopical assessment of the effects of self-healing on the mechanical and durability performance recovery of advanced cementitious composites in extremely aggressive scenarios.

Acknowledgements The activity described in this paper has been performed in the framework of the project "Rethinking coastal defense and Green-energy Service infrastructures through enHancEd-durAbiLity high-performance cement-based materials-ReSHEALience", funded by the European Union Horizon 2020 research and innovation program under GA No 760824 in synergy with the project SMARTINCs, this project has received funding from the European Union's Horizon 2020 research and innovation programme under the Marie Sklodowska-Curie grant agreement No 860006. The information and views set out in this publication are those of the authors and do not necessarily reflect the official opinion of the European Commission. The authors also acknowledge the IDEA League research stay program for research cooperation between Politecnico di Milan and TUDelft. Arjan Thijssen, and Maiko van Leeuwen (Micro lab. TUDelft) are gratefully acknowledged for their technical supports. The authors also acknowledge the IDEA League Research Stay Program for research cooperation between Politecnico di Milano and the Technical University of Delft.

Funding Horizon 2020 Framework Programme, GA 760824, Liberato Ferrara.

References

1. Abbas S, Soliman AM, Nehdi ML (2014) Chloride ion penetration in reinforced concrete and steel fiber-reinforced concrete precast tunnel lining segments. Mater J 111(6):613–622. https://doi.org/10.14359/51686991
2. Pyo S, Koh T, Tafesse M, Kim HK (2019) Chloride-induced corrosion of steel fiber near the surface of ultra-high performance concrete and its effect on flexural behavior with various thickness. Constr Build Mater 224:206–213. https://doi.org/10.1016/J.CONBUILDMAT.2019.07.063
3. Pyo S, Tafesse M, Kim H, Kim HK (2017) Effect of chloride content on mechanical properties of ultra high performance concrete. Cem Concr Compos 84:175–187. https://doi.org/10.1016/J.CEMCONCOMP.2017.09.006
4. Vieira MM, Cavalaro SHP, Aguado A, Rambo DAS, Salvador RP (2021) Fibre corrosion in uncracked high-performance fibre reinforced cementitious composites. Constr Build Mater 312:125440. https://doi.org/10.1016/J.CONBUILDMAT.2021.125440
5. Marcos-Meson V, Michel A, Solgaard A, Fischer G, Edvardsen C, Skovhus TL (2018) Corrosion resistance of steel fibre reinforced concrete—a literature review. Cement Concr Res 103:1–20. https://doi.org/10.1016/j.cemconres.2017.05.016
6. Hashimoto K, Toyoda T, Yokota H, Kono K and Kawaguchi T (2013) Tension-softening behavior and chloride ion diffusivity of cracked ultra high strength fiber reinforced concrete
7. Shin W, Yoo DY (2020) Influence of steel fibers corroded through multiple microcracks on the tensile behavior of ultra-high-performance concrete. Constr Build Mater 259:120428. https://doi.org/10.1016/J.CONBUILDMAT.2020.120428
8. Yoo DY, Shin W, Chun B (2020) Corrosion effect on tensile behavior of ultra-high-performance concrete reinforced with straight steel fibers. Cem Concr Compos 109:103566. https://doi.org/10.1016/J.CEMCONCOMP.2020.103566
9. Yoo DY, Shin W, Banthia N (2021) Corrosion of partially and fully debonded steel fibers from ultra-high-performance concrete and its influence on pullout resistance. Cem Concr Compos 124:104269. https://doi.org/10.1016/J.CEMCONCOMP.2021.104269
10. Yoo DY, Gim JY, Chun B (2020) Effects of rust layer and corrosion degree on the pullout behavior of steel fibers from ultra-high-performance concrete. J Mater Res Technol 9(3):3632–3648. https://doi.org/10.1016/J.JMRT.2020.01.101
11. Marcos-Meson V, Fischer G, Solgaard A, Edvardsen C, Michel A (2020) Mechanical performance and corrosion damage of steel fibre reinforced concrete—a multiscale modelling approach. Constr Build Mater 234:117847. https://doi.org/10.1016/J.CONBUILDMAT.2019.117847
12. Marcos-Meson V et al (2020) Durability of cracked SFRC exposed to wet-dry cycles of chlorides and carbon dioxide—Multiscale deterioration phenomena. Cem Concr Res 135:106120. https://doi.org/10.1016/J.CEMCONRES.2020.106120
13. De Weerdt K, Bernard E, Kunther W, Pedersen MT, Lothenbach B (2023) Phase changes in cementitious materials exposed to saline solutions. Cem Concr Res 165:107071. https://doi.org/10.1016/J.CEMCONRES.2022.107071
14. Ishida T, Iqbal PON, Anh HTL (2009) Modeling of chloride diffusivity coupled with non-linear binding capacity in sound and cracked concrete. Cem Concr Res 39(10):913–923. https://doi.org/10.1016/J.CEMCONRES.2009.07.014
15. Cuenca E, Ferrara L (2017) Self-healing capacity of fiber reinforced cementitious composites. State of the art and perspectives. KSCE J Civ Eng 21(7):2777–2789. https://doi.org/10.1007/s12205-017-0939-5

16. Cuenca E, Tejedor A, Ferrara L (2018) A methodology to assess crack-sealing effectiveness of crystalline admixtures under repeated cracking-healing cycles. Constr Build Mater 179:619–632. https://doi.org/10.1016/j.conbuildmat.2018.05.261
17. Ferrara L, Ferreira SR, Krelani V, Della Torre M, Silva F, Filho RDT (2015) Natural fibres as promoters of autogeneous healing In HPFRCCS: results from on-going Brazil–Italy cooperation. Spec Publ 305:11.1-11.10
18. Lepech MD, Li VC (2009) Water permeability of engineered cementitious composites. Cem Concr Compos 31(10):744–753. https://doi.org/10.1016/j.cemconcomp.2009.07.002
19. Li M, Li VC (2011) Cracking and healing of engineered cementitious composites under chloride environment. ACI Mater J 108(3):333–340. https://doi.org/10.14359/51682499
20. Snoeck D, De Belie N (2016) Repeated autogenous healing in strain-hardening cementitious composites by using superabsorbent polymers. J Mater Civ Eng 28(1):04015086. https://doi.org/10.1061/(ASCE)MT.1943-5533.0001360
21. Gupta S, Al-Obaidi S, Ferraral L (2021) State of the art on self-healing capacity of cementitious materials based on data mining strategies. Spec Publ 350:27–44
22. Gupta S, Al-Obaidi S, Ferrara L (2021) Meta-analysis and machine learning models to optimize the efficiency of self-healing capacity of cementitious material. Materials 14:4437. https://doi.org/10.3390/MA14164437
23. Qiu J (2019) Autogenous healing of fibre/matrix interface and its enhancement. doi: https://doi.org/10.21012/fc10.233115.
24. Banthia N, Foy C (1989) Marine curing of steel fiber composites. J Mater Civ Eng 1(2):86–96. https://doi.org/10.1061/(ASCE)0899-1561(1989)1:2(86)
25. Frazão C, Barros J, Camões A, Alves AC, Rocha L (2016) Corrosion effects on pullout behavior of hooked steel fibers in self-compacting concrete. Cem Concr Res 79:112–122. https://doi.org/10.1016/J.CEMCONRES.2015.09.005
26. de Souza Oliveira A, da Fonseca Martins O, Gomes L, de Ferrara E, Fairbairn MR, Toledo Filho RD (2021) An overview of a twofold effect of crystalline admixtures in cement-based materials: from permeability-reducers to self-healing stimulators. J Build Eng. 41:102400. https://doi.org/10.1016/J.JOBE.2021.102400
27. Cuenca E, Mezzena A, Ferrara L (2021) Synergy between crystalline admixtures and nano-constituents in enhancing autogenous healing capacity of cementitious composites under cracking and healing cycles in aggressive waters. Constr Build Mater 266:121447. https://doi.org/10.1016/j.conbuildmat.2020.121447
28. Cuenca E, D'Ambrosio L, Lizunov D, Tretjakov A, Volobujeva O, Ferrara L (2021) Mechanical properties and self-healing capacity of ultra high performance fibre reinforced concrete with alumina nano-fibres: tailoring ultra high durability concrete for aggressive exposure scenarios. Cem Concr Compos 118:103956. https://doi.org/10.1016/j.cemconcomp.2021.103956
29. Lo Monte F, Ferrara L (2021) Self-healing characterization of UHPFRCC with crystalline admixture: experimental assessment via multi-test/multi-parameter approach. Constr Build Mater 283:122579. https://doi.org/10.1016/J.CONBUILDMAT.2021.122579
30. Lo Monte F, Ferrara L (2020) Tensile behaviour identification in ultra-high performance fibre reinforced cementitious composites: indirect tension tests and back analysis of flexural test results. Mater Struct Constr 53(6):1–12. https://doi.org/10.1617/s11527-020-01576-8
31. Cuenca E, Lo Monte F, Moro M, Schiona A, Ferrara L (2021) Effects of autogenous and stimulated self-healing on durability and mechanical performance of UHPFRC: validation of tailored test method through multi-performance healing-induced recovery indices. Sustainability 13(20):11386. https://doi.org/10.3390/SU132011386
32. Cuenca L, Estefania C, Maria G, Mercedes A, Cruz M, Ferrara, (2022) Effects of alumina nanofibers and cellulose nanocrystals on durability and self-healing capacity of ultrahigh-performance fiber-reinforced concretes. ASCE J Mater Civil Eng. https://doi.org/10.1061/(ASCE)MT.1943-5533.0004375
33. Cuenca E, Postolachi V, Ferrara L (2023) Cellulose nanofibers to improve the mechanical and durability performance of self-healing Ultra-High Performance Concretes exposed to aggressive waters. Constr Build Mater 374:130785. https://doi.org/10.1016/J.CONBUILDMAT.2023.130785
34. Davolio M, Al-Obaidi S, Altomare MY, Monte FL, Ferrara L (2023) A methodology to assess the evolution of mechanical performance of UHPC as affected by autogenous healing under sustained loadings and aggressive exposure conditions. Submitt Publ Cem Concr Compos 139:105058
35. L. XI, B., Huang, Z., Al-Obaidi, S. and Ferrara, "Predicting High-Performance Concrete (UHPC) self-healing performance using hybrid models based on metaheuristic optimization techniques," *Submitt. Publ. to Constr. Build. Mater.*
36. Cuenca E, Ferrara L (2020) Fracture toughness parameters to assess crack healing capacity of fiber reinforced concrete under repeated cracking-healing cycles. Theor Appl Fract Mech. https://doi.org/10.1016/j.tafmec.2019.102468
37. Xue C, Li W, Luo Z, Wang K, Castel A (2021) Effect of chloride ingress on self-healing recovery of smart cementitious composite incorporating crystalline admixture and MgO expansive agent. Cem Concr Res 139:106252. https://doi.org/10.1016/J.CEMCONRES.2020.106252
38. Wille K and Naaman AE (2010) Bond stress-slip behavior of steel fibers embedded in ultra high performance concrete. In: 18th European Conference on Fracture: Fracture of Materials and Structures from Micro to Macro Scale, p 111
39. Wille K, Naaman AE (2013) Effect of ultra-high-performance concrete on pullout behavior of high-strength brass-coated straight steel fibers. Mater J 110(4):451–462. https://doi.org/10.14359/51685792
40. Marcos-Meson V, Solgaard A, Hjorth Jakobsen U, Edvardsen C, Fischer G, Michel A (2021) Pull-out behaviour of steel fibres in cracked concrete under wet-dry cycles-deterioration phenomena. Mag Concr Res. https://doi.org/10.1680/jmacr.19.00448
41. Marcos-Meson V, Solgaard A, Fischer G, Edvardsen C, Michel A (2020) Pull-out behaviour of hooked-end steel fibres in cracked concrete exposed to wet-dry cycles of

chlorides and carbon dioxide—Mechanical performance. Constr Build Mater. https://doi.org/10.1016/J.CONBUILDMAT.2019.117764
42. Feng H, Sheikh MN, Hadi MNS, Feng L, Gao D, Zhao J (2019) Pullout behaviour of different types of steel fibres embedded in magnesium phosphate cementitious matrix. Int J Concr Struct Mater 13(1):1–17. https://doi.org/10.1186/S40069-019-0344-1/TABLES/5
43. Abdallah S, Fan M, Rees DWA (2017) Effect of elevated temperature on pull-out behaviour of 4DH/5DH hooked end steel fibres. Compos Struct 165:180–191. https://doi.org/10.1016/J.COMPSTRUCT.2017.01.005
44. Naaman AE, Najm H (1991) Bond-slip mechanisms of steel fibers in concrete. Mater J 88(2):135–145. https://doi.org/10.14359/1896
45. Oh T, You I, Banthia N, Yoo DY (2021) Deposition of nanosilica particles on fiber surface for improving interfacial bond and tensile performances of ultra-high-performance fiber-reinforced concrete. Compos Part B Eng 221:109030. https://doi.org/10.1016/J.COMPOSITESB.2021.109030
46. Bentur A, Diamond S, Mindess S (1985) The microstructure of the steel fibre-cement interface. J Mater Sci. https://doi.org/10.1007/BF01113768
47. Bentur A, Mindess S (2006) Fibre reinforced cementitious composites. CRC Press, London
48. Marcos-Meson V, Solgaard A, Fischer G, Edvardsen C, Michel A (2020) Pull-out behaviour of hooked-end steel fibres in cracked concrete exposed to wet-dry cycles of chlorides and carbon dioxide—Mechanical performance. Constr Build Mater 240:117764. https://doi.org/10.1016/j.conbuildmat.2019.117764
49. Marcos-Meson V, Fischer G, Solgaard A, Edvardsen C, Michel A (2021) Mechanical performance of steel fibre reinforced concrete exposed to wet–dry cycles of chlorides and carbon dioxide. Materials. https://doi.org/10.3390/ma14102642
50. Sisomphon K, Copuroglu O, Koenders EAB (2012) Self-healing of surface cracks in mortars with expansive additive and crystalline additive. Cem Concr Compos 34(4):566–574. https://doi.org/10.1016/J.CEMCONCOMP.2012.01.005
51. Kim S, Choi S, Yoo DY (2020) Surface modification of steel fibers using chemical solutions and their pullout behaviors from ultra-high-performance concrete. J Build Eng 32:101709. https://doi.org/10.1016/J.JOBE.2020.101709